JOURNAL OF MATERIALS SCIENCE 29 (1994) 1–10

Chemical interaction during the chemical vapour deposition of silicon carbide on aluminosilicate fibres from halogenated precursors

C. VINCENT, J. P. SCHARFF, H. VINCENT, J. BOUIX, N. LOFTI, T. S. KANNAN*
Laboratoire de Physicochimie Minérale I, Université Claude Bernard, 43, Boulevard du 11 Novembre 1918, 69622 Villeurbanne Cedex, France

Preliminary studies on the coating of silicon carbide (β-SiC) on aluminosilicate fibres of the type Nextel by chemical vapour deposition (CVD), at atmospheric pressure, are reported. Classical CVD experiments were performed by using various precursor gases, such as silicon tetrachloride–methane–hydrogen, methyltrichlorosilane (MTS)–hydrogen and dimethyl dichlorosilane (DDS)–hydrogen mixtures. The deposition processes were studied by thermodynamic calculations. The SiC texture is dependent on the precursor used. It is shown that the best results are obtained from DDS–H_2 mixture; the deposit covers the filaments, but has a columnar growth commonly found in CVD materials. The mechanical properties of the different fibres, such as tensile strength and Young's modulus, were monitored at each stage before and after every coating. The decrease of σ_R is attributed to the high temperatures which modify the structure of the fibre and to attack the silicoaluminate substrate by the gas mixture with 1σSS of $AlCl_3$, rather than the SiC coating.

1. Introduction

The improvement of mechanical properties of ceramic materials by high-strength refractory fibre reinforcement, especially for high-temperature applications, has resulted in the emergence of ceramic composite materials that could possibly find application in automobile heat engines, aeronautical and aerospace structural components, machine tools and wear-resistant parts, etc. The production of matrix-compatible coatings on a variety of high-strength fibres is the general objective of the work in our laboratory [1–6]. We report here some of the studies carried out on the coating of silicon carbide on aluminosilicate fibres, commercially known as Nextel. The coatings are also expected to offer a non-chemically interactive diffusion barrier between the matrix and the fibres during sintering of the composite powders. Direct sintering or hot pressing of alumina powders together with silicoaluminate fibres are known to lead to extensive reaction and interdiffusion leading to the disappearance of the fibres during sintering [7]. Thus, an intermediate layer of some other non-reactive material coating, such as SiC, on these fibres seems to be required, because silicon carbide is known to be compatible with both mullite and alumina [8]. Further, because its thermal expansion coefficient ($3.8 \times 10^{-6}\,°C^{-1}$ [9]) is close to that of Nextel fibres ($3.5 \times 10^{-6}\,°C^{-1}$ [10]) this should help in decreasing thermal constraints during fabrication of the composite. The chemical vapour deposition (CVD) of β-SiC on inert substrates has been the subject of a large number of investigations [1–16]. It is shown that, depending on the gas mixtures and their relative composition, the deposition temperature and the total pressure of deposition, widely varying results can be obtained. Schlichting [12, 13] has briefly summarized the results of the earlier studies. In the case of oxide substrates, recent results have shown that alumina and mullite were not chemically inert in the presence of halogenated precursors, and a strong interaction is possible. The magnitude of this attack and the morphology of the SiC deposit are dependent on the type of the precursor system and the deposition conditions [6].

One objective of this study was to determine if the CDV process could be used to produce an SiC deposit on silicoaluminate fibres, continuously and at atmospheric pressure; the other objective was to determine the experimental conditions which retain the mechanical properties of the fibres at a reasonably high level for their use in a ceramic matrix. In the present work, the SiC coating was produced by chemical vapour deposition from $SiCl_4$–CH_4–H_2 mixture and from different chlorosilanes, methyltrichlorosilane (MTS) and dimethyldichlorosilane (DDS). The experiments were preceded by thermodynamic calculations.

* *Present address:* National Aeronautical Laboratory, Bangalore, India.

0022–2461

2. Thermodynamic calculations

An accurate knowledge of the gas phase and solid-phase composition of such a complex chemical system is of prime importance to assess the deposition efficiency as a function of CVD parameters and is a first step in the understanding of the kinetic processes.

A theoretical approach based on the calculation of equilibrium thermodynamic compositions of the various species in the Si–C–H–Cl system has been attempted recently by Kingon *et al.* [17] and by Christin *et al.* [18]. In the case of oxide substrates, the gas phase reacts with the solid, and the conclusions of these calculations are not viable. For the SiC CVD on an oxide substrate, it is important to determine the conditions which permit the formation of the solid single-phase of SiC, a high conversion of precursor into SiC and the reduction of the substrate degradation.

In this work, we present the results of thermodynamic calculations relating to the Al–O–Si–C–Cl–H system for a total pressure of 1 atm. The calculations were planned according to the free-energy minimization method. They were performed by supposing the presence of 34 gas species, 2 liquid species and 9 solid species, which are indicated in Table I. The thermodynamic data for these species were taken from Janaf tables [19]. The tables give graphite as the stable condensed form of carbon, and β-SiC a lower free energy than the α-form at all temperatures; only these forms are considered in the calculations, and the experiments support this choice. The aluminium oxycarbides, Al_2OC and Al_4O_4C, and the mixed carbides, Al_4SiC_4, Al_8SiC_7 and $Al_4Si_2C_5$, are not envisaged in this study because of their instability or their low formation kinetics [20–24]. At high temperatures, DDS is not stable, and we have considered only the Al_2O_3–$SiCl_4$–CH_4–H_2 system and the Al_2O_3–MTS–H_2 system, where Al_2O_3 is in excess. For both systems the calculations were performed in the range temperature 1300–1500 K and for all the calculations; the initial mole numbers of Al_2O_3 and $SiCl_4$ (or MTS) are kept constant, respectively equal to 5 and 2 mol. The relative compositions of the input gas mixtures are expressed in the form of the A and D ratios where $A = Si/(Si + C)$ and $D = H_2/(Si + C)$.

TABLE I Chemical species, gaseous and condensed, in the thermodynamic calculations

Solid species	C(gr.), Si, Al, β-SiC, SiO_2, Al_4C_3, α-Al_2O_3, $Al_2O_7Si_2$, $Al_6O_{13}Si_2$ (mullite)
Liquid species	Si, Al
Gas species	Si, SiCl, $SiCl_2$, $SiCl_3$, $SiCl_4$, SiH_3Cl, SiH_2Cl_2, $SiHCl_3$, $SiCH_3Cl_3$, SiH, SiH_4, CH_3, CH_4, C_2H_2, C_2H_4, $CHCl_3$, CH_2Cl_2, CH_3Cl, CCl_4, CO_2, CO, Al, AlCl, $AlCl_3$, Al_2Cl_6, $AlHO_2$, HCl, Cl, Cl_2, ClO_2, Cl_2O, H_2, H, H_2O

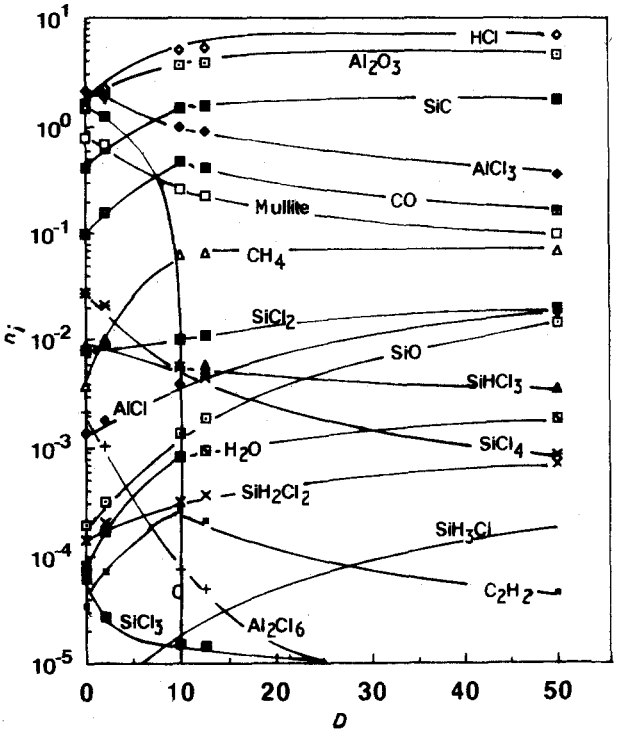

Figure 1 CVD of SiC from Al_2O_3–$SiCl_4$–CH_4–H_2 system. Effect of varying the D ratio on the mole number of the main species at equilibrium for a total pressure of 1 atm and an equimolecular $SiCl_4$–CH_4 mixture ($A = 0.5$).

2.1. Al_2O_3–$SiCl_4$–CH_4–H_2 system

The calculation programme was applied essentially to the cases: $A = 0.5$ and 0.8. Fig. 1, by way of example, shows results for $A = 0.5$ and $T = 1500$ K. The equilibrium composition is given as a function of the D ratio. The main species are Al_2O_3, $3Al_2O_3$–$2SiO_2$ (mullite), β-SiC, $AlCl_3$, C, Si, $SiCl_4$, H_2, HCl, and CO, $AlCl_3$ and mullite are the products of attack of Al_2O_3 by $SiCl_4$–H_2 mixtures. The existence domains of the solid species formed are given in Fig. 2. For an easier interpretation of CVD parameter influence on the β-SiC formation, and also on the extent of the attack of Al_2O_3, we have only considered the evolution of $AlCl_3$ and the solid species in Figs 3 and 4. In particular, curves SiC and Si give the amounts of silicon feed converted into solid. In both cases ($A = 0.5$ and 0.8), SiC yields decrease with increasing D. Carbon appears in equilibrium products; however, the calculations show that there is an upper limit to the carbon formation for a specific D ratio, this limit is depending on the A ratio and the temperature. The appearance of carbon may be avoided by using an $SiCl_4$–H_2 mixture rich in hydrogen. In the case of $A = 0.8$, the favourable effect of D is not evident, because solid silicon can be formed for the high hydrogen gas concentrations.

The different figures show that Al_2O_3 reacts with the initial gas phase to give mullite and $AlCl_3$; this result is in agreement with the earlier experiments [6]. The data show that the reaction between Al_2O_3 and the input gas mixture diminishes with a lowering of the A ratio and an increase in the temperature. Also, one may note a progressive decrease of Al_2O_3 attack as D increases. It thus appears that high temperatures (1500 K), $A = 0.5$ and $D > 20$ may be of certain interest for the CVD coating on Al_2O_3 fibres substrates.

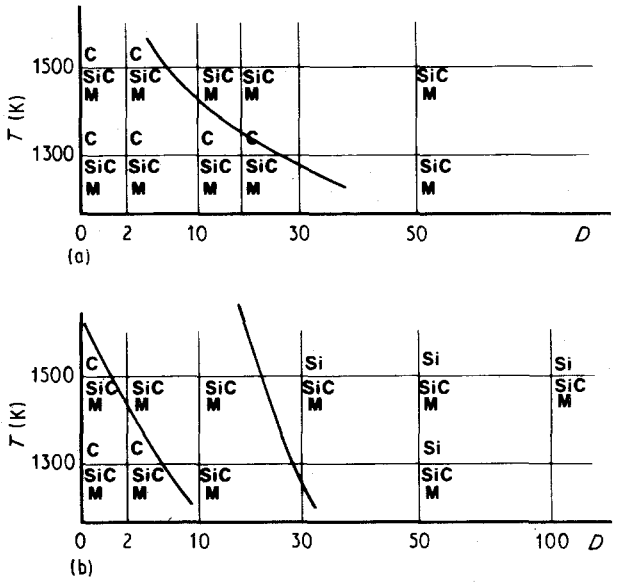

Figure 2 The Al_2O_3–$SiCl_4$–CH_4–H_2 system at atmospheric pressure. CVD phase diagram [$(D = H_2/(Si + C)$, $A = Si/(Si + C)$]. (a) $A = 0.5$, (b) $A = 0.8$. M = mullite.

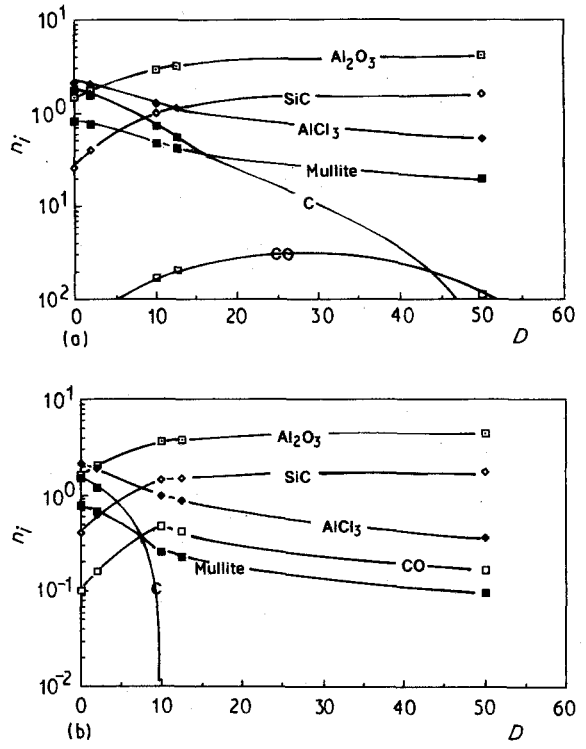

Figure 3 The Al_2O_3–$SiCl_4$–CH_4–H_2 system. Variation of mole numbers for the main species as a function of D, at $P = 1$ atm and $A = 0.5$. (a) $T = 1300$ K, (b) $T = 1500$ K.

2.2. MTS–H_2 system

In this system, the A ratio was fixed at 0.5. In all the envisaged cases, the calculations show that Al_2O_3 reacts with the MTS–H_2 mixture to give mainly $AlCl_3$ gas and mullite solid. The CVD phase diagram is reported in Fig. 5. In this diagram, phase fields of β-SiC and β-SiC + C are observed. If one desires to elaborate the single-phase β-SiC, one should work at high hydrogen carrier gas concentration and at high temperature.

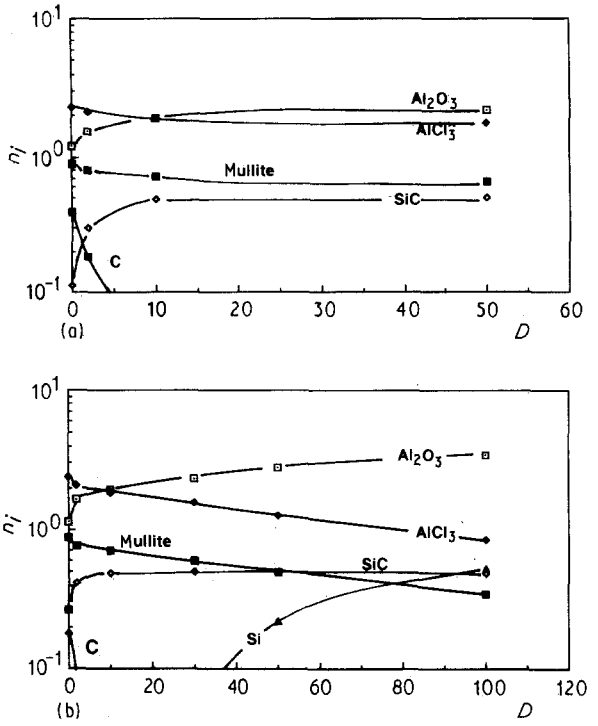

Figure 4 The Al_2O_3–$SiCl_4$–CH_4–H_2 system. Variation of mole numbers for the main species as a function of D, at $P = 1$ atm and $A = 0.8$. (a) $T = 1300$ K, (b) $T = 1500$ K.

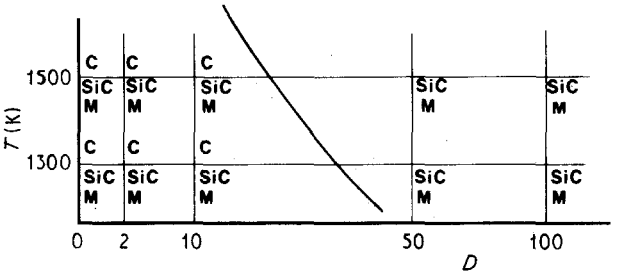

Figure 5 The Al_2O_3–MTS–H_2 system at $P = 1$ atm, A = 0.5.

For the SiC CVD on Al_2O_3 substrates, the differences in behaviour between $SiCl_4$–CH_4–H_2 mixture and MTS–H_2 mixture is not negligible. For example, the limit between the two fields, β-SiC + C and SiC, shifts with changing precursor. At high hydrogen carrier gas concentrations, this system is very similar to that of $SiCl_4$–CH_4–H_2 discussed above; at low hydrogen concentration, the equilibrium compositions are different, in particular, the amount of Al_2O_3 converted into $AlCl_3$ is reduced when MTS is used (Fig. 6)

2.3. Conclusion and comparison with earlier experimental data

Although β-SiC is deposited under all conditions, codeposition of carbon or silicon and attack of Al_2O_3 are the dominant features of the thermodynamical calculations. The necessity for high hydrogen carrier gas concentrations is apparent to maximize deposition efficiency and minimize the attack of Al_2O_3. For the low hydrogen carrier gas concentration, the present

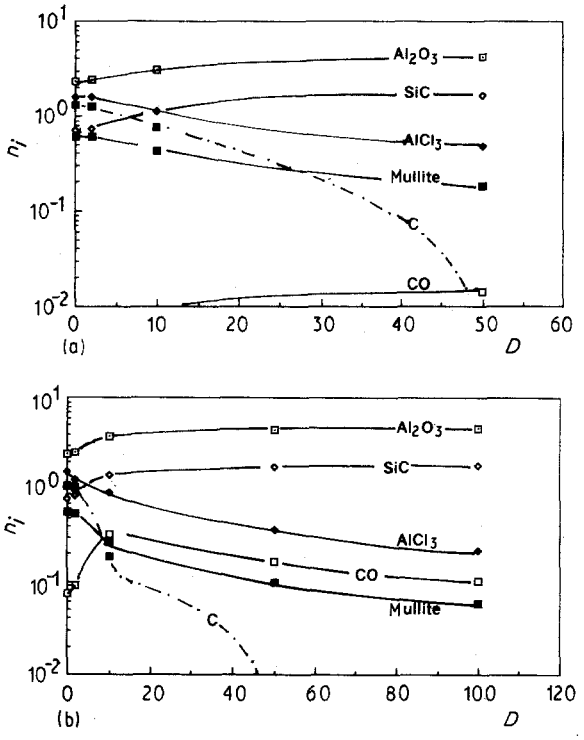

Figure 6 The Al_2O_3–MTS–H_2 system at $P = 1$ atm. Variation of mole numbers for the main species as a function of D. (a) $T = 1300$ K, (b) $T = 1500$ K.

results show that the MTS–H_2 system is substantially different from this which contains $SiCl_4$. Moreover, it seems that the magnitude of Al_2O_3 degradation depends on the chlorine concentration in the input gas. Experimental work recently reported [6] is easily compared with the present results. A good agreement between experimental and calculated results is obtained (Fig. 7).

3. Experimental procedure

The characteristics of Nextel fibres are presented in Table II [18]. The purpose of this study was to produce a thin coating on the fibres by a continuous process and to determine the evolution of the mechanical characteristics as a function of the CVD parameters. The treatment time was less than 1 min, therefore, the results can differ from those obtained on bulky substrates. Based on the thermodynamic conclusions of CVD of SiC on alumina substrates and on the experimental results on plate substrates of alumina and mullite [6], the experiments of SiC deposition on Nextel fibres were limited to the following precursor systems:

(i) silicon tetrachloride ($SiCl_4$)–methane (CH_4)–hydrogen (H_2)
(ii) trimethylchlorosilane (TMS)–hydrogen (H_2)
(iii) dimethyldichlorosilane (DDS)–hydrogen (H_2)

We present here a detailed study of the CVD of silicon carbide on Nextel-312 fibres and some preliminary studies on the CVD of Nextel-440 fibres using silicon tetrachloride–methane–hydrogen as the precursor mixture.

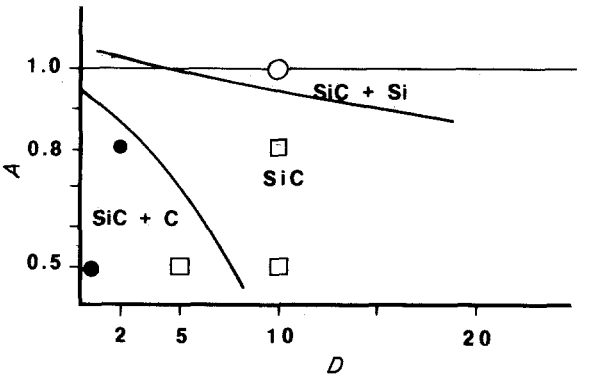

Figure 7 Comparison between thermodynamical and experimental data. The limits of phase domains are calculated from minimization of free energy. The marked points correspond to experimental results on massive alumina substrate [6] and characterization by XRD. (●) C, (○) Si, (□) SiC.

TABLE II Properties of the Nextel fibres

	Nextel-312	Nextel-440	Nextel-480
Strand diameter (μm)	10–12	10–12	10–12
Number of strands	780	780	780
Density (mg cm^{-3})	2.7–2.9	3.05	3.05
Rupture strength (MPa)	1700	2000	1900
Young's modulus (GPa)	150	190	220
Specific surface (m^2 mg^{-1})	< 0.2	< 0.2	< 0.2
Chemical composition:			
Al_2O_3(%)	62	70	70
SiO_2(%)	24	28	28
B_2O_3(%)	14	2.0	2.0

3.1. CVD apparatus and characterization methods

With the exception of hydrogen and methane, the other precursors (silicon silicon tetrachloride, methyltrichlorosilane and dimethyldichlorosilane) are liquid at room temperature. These chloride compounds possess a high vapour pressure ($SiCl_4$ 228 mm Hg, MTS 250 mm Hg and DDS 167.5 mm Hg, at 25 °C) for being transported in the CVD reactor by hydrogen as a carrier gas.

The gas distribution/supply system was described in an earlier publication [6]. Hydrogen gas itself, at a predetermined rate, was used as a carrier gas for the halosilane transport; it was passed through a vessel containing the liquid chloride, the amount of chloride carried being dependent upon the vapour pressure of the liquid. The mixture before entering the reactor joined a direct stream of hydrogen of the desired flow rate and was thoroughly mixed with it. Calibrated flow meters (Brook's Instruments) were used to measure and control the flow rates and thereby the quantity of precursors admitted into the reactor.

A schematic diagram of the CVD reactor is shown in Fig. 8. The reactor consists of a silica tube (22 mm inner diameter) which at either end fits a stainless steel flange. The flanges contain stainless steel pulleys (5 cm diameter) which are driven by two motors for the transport of fibres. The device permits the fibres to be

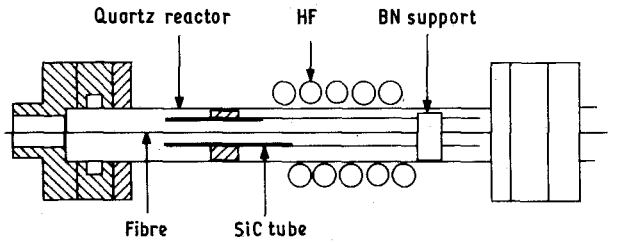

Figure 8 Schematic diagram of the CVD reactor used for continuous fibre coating.

transported in two directions, at a rate varying from 0–60 cm min^{-1}. For the CVD treatment, the fibres were always transported in a direction opposite to that of the gas flow. They were heated by induction using a hollow SiC rod (60 cm length) as a susceptor. An optical pyrometer was used to measure the temperature of the susceptor during the CVD experiments. The temperature of the fibres was calibrated using a thermocouple fixed to the fibres; a uniform temperature of 1200 °C could be obtained over a length of 30 cm. The treatment time was defined by the ratio between 30 cm and the fibre transportation rate.

All the commercial Nextel fibres (Nextel-312, 440, 480) contain a protective sizing and must be subjected to a cleaning operation before coating with SiC. In this study, we have evolved several methods to remove the sizing; the dissolution in organic solvents is much less effective than heat treatments in an argon atmosphere. We have tested different temperatures and different durations; after each treatment, the filament morphology, the fibre crystallization and the tensile strength were compared with the properties of the initial fibre. At low temperature ($T < 800$ °C) the requisite time is several hours; at high temperature, some seconds are adequate, and the cleaning can be carried out in the reactor by transport of the fibres at 60 cm min^{-1} from one pulley to the other, at 1050 °C.

Physical characterization of the fibres was done using X-ray diffraction (XRD, Philips diffractometer, CuK_α). The XRD characterization of the Nextel fibres was made using finely ground or aligned fibres. The obtained spectra are shown in Fig. 9a–c; the β-SiC spectra is shown for comparison (Fig. 9d). While Nextel-312 gives an amorphous pattern, Nextel-440 and 480 give patterns which correspond to partially crystallized phases, that of Nextel 480 corresponding more closely to mullite.

Raman spectroscopy (Jobin-Yvon spectrometer, $I = 488$ nm) is a complementary technique, it was used to identify the chemical nature of the amorphous deposit and to confirm the XRD results. The spectrometer is equipped with a microscope which focused the laser beam on a filament surface, the area of the analysed surface is around 1 mm^2. The scattered light is collected on the entrance slit (500 μm) of a double monochromator; the instrumental resolution is 20 cm^{-1}.

The surface topology and fibre cross-sections were investigated using Hitachi and Jeol scanning electron microscopes.

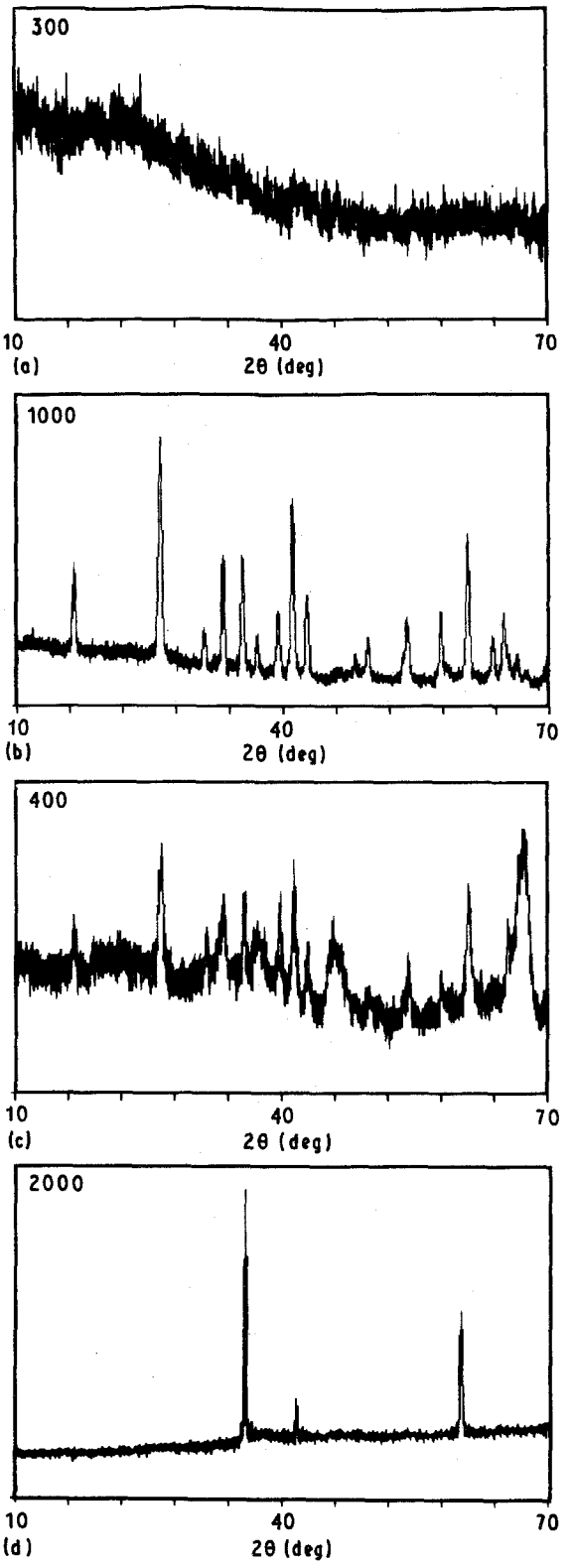

Figure 9 XRD patterns of reference materials. (a) Nextel-312, (b) Nextel-440, (c) Nextel-480, (d) β-SiC.

The main interest in the Nextel fibres as a reinforcing agent for composite fabrication is based on their high values of rupture strength, σ_R, as can be seen from Table II. Because subsequent heat treatments and CVD could alter these values, we measured the rupture tensile strength and the Young's modulus, E, of these fibres before and after each treatment by subjecting 20 mm long single filaments to tensile traction tests in a Adamel DY-22 machine equipped with

a load cell of 500 cN. The crosshead displacement speed was 0.1 mm min^{-1}. Tensile tests were performed on at least 30 single filaments of each type to subject the results to Weibull statistics in order to obtain reliable values of rupture strength, as well as the Weibull parameter, m, after each treatment given to the fibres. The Young's modulus was obtained from the slope of the load–displacement curves of the single filaments. The calculation of the rupture strength and Young's modulus requires the average diameter of the fibre to be known fairly accurately. For this purpose, the fibres were cut and fixed in a small vice which could be kept inside the SEM. The cross-sectional diameters were measured for a number of fibres and, for Nextel-312, an average value of 10.7 9m was obtained. We have assumed this value of 10.7 μm for the average diameter of the fibres for our calculations.

3.2. Continuous deposition of SiC on Nextel fibres

The fibres after initial heat cleaning were first wound on one pulley. They were transported through the furnace at 1050 °C for the final removal of the sizing layer. The reactor was then evacuated and hydrogen was admitted and allowed to flow for 15 min. This was followed by the flow of precursor mixtures and the transport of the fibre to the opposite end under the temperature required for the SiC CVD. The pulley speeds were monitored to obtain a reaction time of 23–46 s for one reactor length of fibres to be coated.

The removal of sizing on the surface is effected before the CVD treatment. Scanning electron microscopy was used to observe the surface features of the fibres. Fig. 10 shows typical electron micrographs of the fibre surface coated with a polymeric sizing and it can be observed that the surface contained a considerable number of defects such as weldings of filaments. With a view to achieving fibre cleaning in a continuous way, we followed a procedure using high temperatures. This heat treatment involves structure modifications of the fibre. In the case of the Nextel-312, which is initially amorphous, the X-ray diffraction peaks became sharp with increasing heat-treatment temperature. The effect of the heat treatment followed by XRD is shown in Fig. 11a and b. At 800 °C, the crystallization commences after 64 h and seemed to be completed after 89 h. However, at 1050 °C, the same crystallization seemed to be effected in just 20 s in the reactor. In the case of Nextel-440 fibres, the crystallization was more rapid than that of Nextel-312. The formation of a completely crystallized mullite phase was not achieved until 1500 °C was reached. After the heat cleaning at 800 °C for 12 h or at 1050 °C for 20 s, the fibre was white, all the filaments of the two were separated and there were few surface defects, as shown in Fig. 12.

A representative example of the Weibull plot for Nextel-312 fibres for rupture strengths obtained by tensile traction experiments is shown in Fig. 13. The

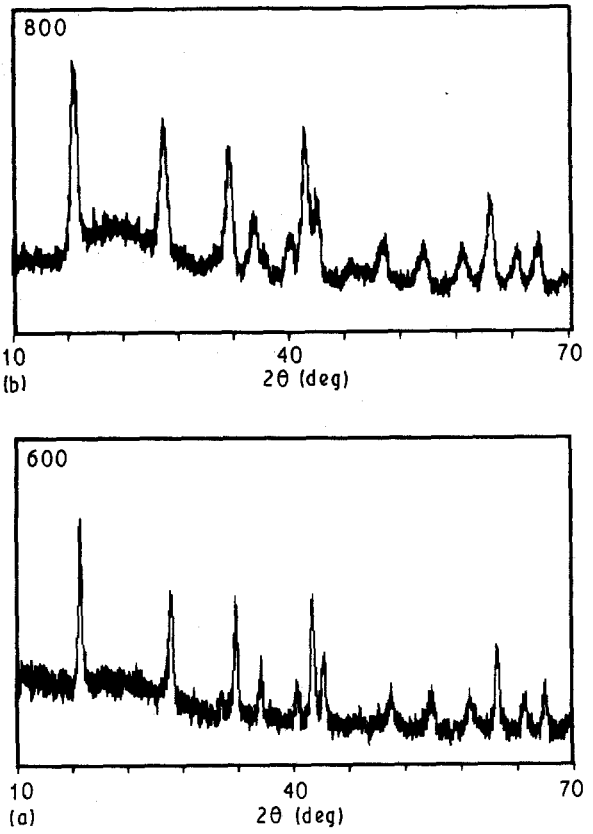

Figure 11 XRD patterns of Nextel-312 after heat treatment to remove the sizing: (a) at 800 °C for 89 h, (b) at 1050 °C for 23 s.

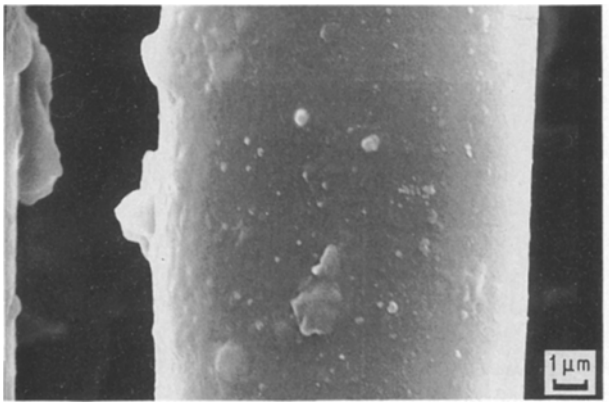

Figure 10 Scanning electron micrograph of Nextel-312 before cleaning.

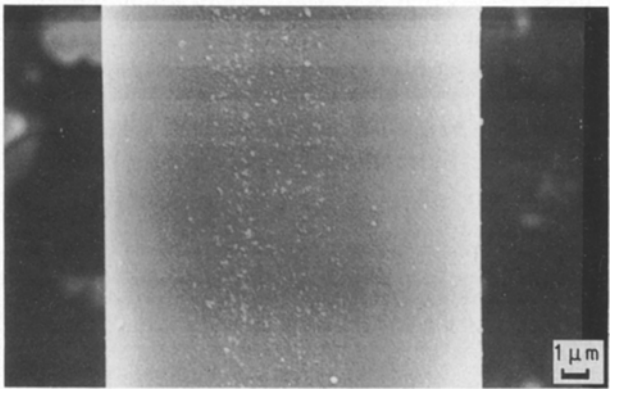

Figure 12 Scanning electron micrograph of Nextel-312 after heat cleaning at 1050 °C for 23 s.

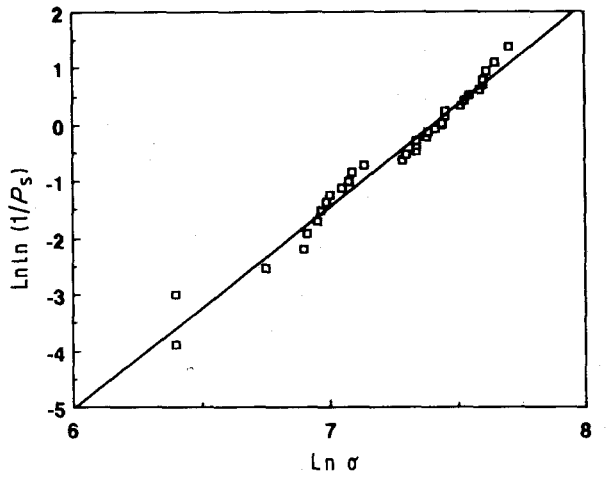

Figure 13 Weibull analysis for Nextel-312: Inln $(1/P_s)$ versus lnσ; Weibull plots.

plots are similarly obtained for the fibres after every treatment to assess the changes to the mechanical properties of the fibres. The results are presented in Table III. The initial values obtained for the rupture strength (1480 MPa) of the Nextel-312 fibres agreed fairly well with that stated by the manufacturers (1700 MPa). Table III also gives the values of rupture strength, σ_R, Young's modulus, E and the Weibull parameter, m, for the fibres after heat treatment. It can be seen that while the rupture strength of the fibres decreases both with temperature and time of heat treatment, the Young's modulus shows a slightly increasing trend. The reason for this behaviour is at presently not very evident. A significant fall in Weibull parameter from 3.6 to 2.2 was also observed. The deterioration in strength occurring at 1050 °C and above, is associated with crystallization of the structure.

3.2.1. Deposition of SiC on Nextel fibres by CVD procedures

The deposition temperature was restricted to 1370 K because the fibres were not able to withstand much higher temperatures (immediate defibrillation, brittleness and breaking of the fibres was noticed at higher temperatures).

3.2.2. SiC CVD on Nextel-440 fibres using $SiCl_4$–CH_4–H_2 and MTS–H_2 as precursor gas mixtures

The experimental conditions are summarized in Table IV. They are similar to those which were used for the previous calculations: however, the A ratio was limited to 0.5 for comparison between the two types of precursor, the D value varying from 2.5–20. The fibre speed was fixed to 1 m min^{-1} which corresponds to a CVD time of 20 s.

After CVD treatment, the characterization showed no appreciable difference between the fibres coated from both precursors: they were dark and a loss of

TABLE III Variation of mechanical characteristics of the Nextel-312 fibres as a function of heat treatment, in air and at atmospheric pressure

Heat treatment	Rupture strength (MPa)	Young's modulus (GPa)	Weibull parameter
initial	1480	95	3.6
800 °C, 6 h	1620	110	4.2
800 °C, 64 h	1100	120	2.9
800 °C, 156 h	660	110	3.2
1050 °C, 28 s	1150	120	2.2

TABLE IV Experimental conditions for SiC CVD from $SiCl_4$–CH_4–H_2 and MTS–H_2 mixtures, at $T = 1370$ K and $P = 1$ atm [$D = H_2/(SiC + C)$, $A = Si/(Si + C)$]

Precursor	A	D	d_t (cm^3 min^{-1})	t (s)	Colour
$SiCl_4$–CH_4–H_2	0.5	2.5	286	20	Dark
$SiCl_4$–CH_4–H_2	0.5	10	436	20	Brown
$SiCl_4$–CH_4–H_2	0.5	20	420	20	Brown
MTS–H_2	0.5	2.5	246	20	Dark

TABLE V Experimental conditions for SiC CVD from DDS–H_2 mixture at $T = 1270$ K and $P = 1$ atm [$D = H_2/(SiC + C)$, $A = Si/(Si + C)$]

Precursor	A	D	d_t (cm^3 min^{-1}	t (s)	Colour	d_{tex} (gm^{-1})
DDS–H_2	0.33	20	227	42	Dark	0.2210
DDS–H_2	0.33	20	227	31	Grey	0.2133
DDS–H_2	0.33	20	227	8	Grey	0.1950

weight was observed. This last result is in agreement with that obtained on a bulky substrate [6]. The SiC deposits is not continuous and does not form a protective layer, thus attack of the fibre is important with the formation of $AlCl_3$ as, a clear deposit observed on the reactor walls. The reaction is

$$2Al_2O_{3(s)} + 3SiCl_{4(g)} \rightarrow 4AlCl_{3(g)} + 3SiO_{2(s)} \quad (1)$$

The filaments became very brittle and no mechanical measurements could be made on them. Because of these problems, further experiments with these precursor systems were discontinued.

3.2.3. Deposition of SiC on Nextel-312 fibres using DDS–H_2 precursor mixture

The conditions optimized earlier [6] for the CVD of silicon carbide on massive alumina and mullite substrates using this precursor were employed in this study. For all the experiments, the A ratio was fixed at 20 and the CVD times were varied from 8–42 s. The experimental conditions used are given in Table V. On leaving the reactor, the fibres had a uniform grey colour, but, with longer dwell times in the reactor, the fibres became dark green, rigid, brittle and were easily susceptible to breaking. The gain in the weight of the fibres was evidence of a poor attack.

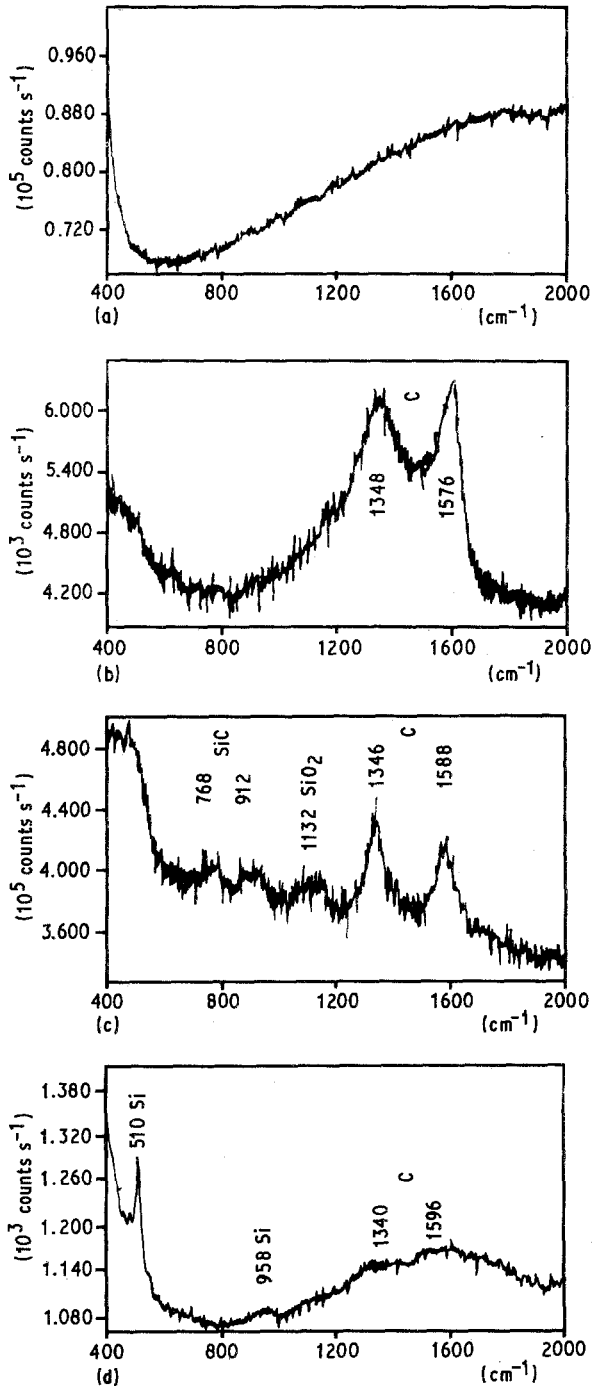

Figure 14 Raman spectra of the coating obtained from the $SiCl_4$–CH_4–H_2 system at 1370 K for 20 s on Nextel-440: (a) after heat treatment, (b) $A = 0.5$ and $D = 2.5$, (c) $A = 0.5$ and $D = 10$, (d) $A = 0.5$ and $D = 20$.

3.3. Characterization

3.3.1. Raman spectroscopy

The Raman spectra of the coated fibres are given in Fig. 14, the spectrum of the initial fibre is also shown for comparison. They are characterized by three series of lines, more or less intense according to the precursor and the gas composition used. With $SiCl_4$–CH_4–H_2 as reactive gas phase, and for $A = 0.5$ and $D = 2.5$, the spectra consist of one series of two strong lines at 1350 and 1600 cm^{-1} due to pyrocarbone (Fig. 14b); these lines are very broad and the expected SiC is not detected by this technic. For $D = 10$, the spectra exhibit five lines, Fig. 14c; the lines at 770 and 910 cm^{-1} are characteristic of β-SiC [25], the two lines at 1350 and 1600 cm^{-1} show that carbon is also present in the coating; the broad line at 1130 cm^{-1} can be attributed to SiO_2. For $D = 20$, the spectra in the Fig. 14d consist mainly of just a sharp line at 510 cm^{-1} which we assigned to silicon, supported by the faint line at 960 cm^{-1} [26]; for this gas composition, carbon is less organized as is supported by a wide broadening of its characteristic lines. It is thus seen that the spectrometry results are not in perfect agreement with the thermodynamic calculations. In the coating, carbon is present as expected for the low value of D; on the contrary, for high D values, silicon formation is only expected from the calculations for the mixture richer in hydrogen than $A = 0.5$; one explanation may be that the composition of the reactive gas which must diffuse in the boundary layer, is different from that introduced into the reactor. Finally, we never obtained single phase β-SiC. With DDS–H_2 mixture as precursor gas and for $D = 20$, the Raman microanalysis proved that the coating was a β-SiC–C mixture. In this case, there was no discrepancy between experiments and theory.

3.3.2. XRD analysis

The XRD patterns of the fibres treated for 31 s in the CVD reactor are shown in Fig. 15. For the detection of β-SiC, carbon or silicon on the surface of the fibre, the use of XRD is complicated by the presence of several peaks of crystallization of aluminosilicates in close vicinity to those of these different compounds. However, it is possible to distinguish the presence of SiC on the analysed fibre by more careful observation of the peak shapes in the region of 34°–38° 2θ.

3.3.3. SEM examination

The scanning electron micrographs of the fibre surface after CVD treatment are shown in Fig. 16. For these examples, the presence of β-SiC is confirmed by XRD and Raman spectroscopy. The topologies differ according to the precursor used. From $SiCl_4$–CH_4–H_2 mixture, the coating was inhomogeneous and poorly adherent; complications including the presence of tiny crystals, whiskers and the deposition of silicon carbide

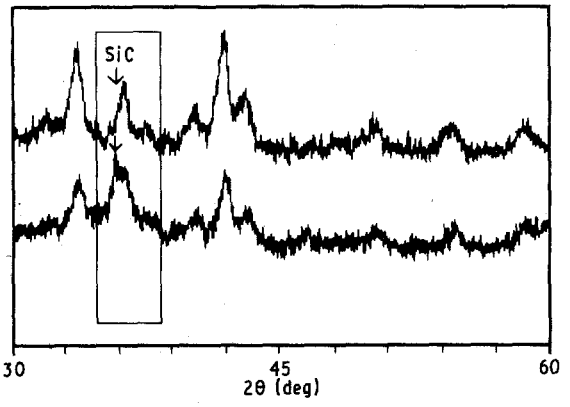

Figure 15 XRD pattern of Nextel-312 coated from DDS–H_2 mixture at 1270 K for 31 s.

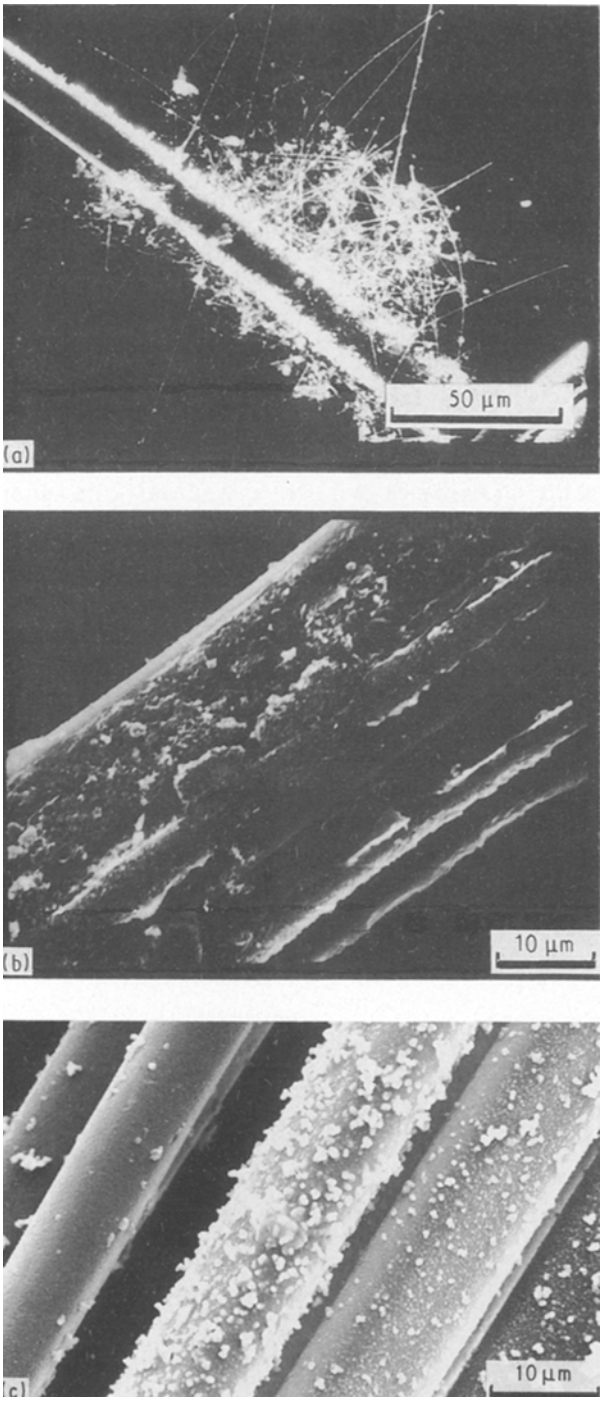

Figure 16 Scanning electron micrograph of the filament surface coated from (a, b): the $SiCl_4$–CH_4–H_2 system, (c) the DDS–H_2 system.

encompassing several filaments at the same time, are also evident from the same photos (Fig. 16a and b). From DDS–H_2 mixture, the SiC coating obtained was continuous and had a granular grain structure (Fig. 16c). This last structure is commonly found in CVD materials, it can result from the growth and aggregation of SiC particles which are formed in the gas phase.

3.4. Mechanical properties

The fibres are brittle and only the SiC fibres produced using DDS–H_2 mixture were tested. Although the attack of the fibre was poor, the value of tensile strength remains very low (800 MPa). Fig. 17 gives the Weibull plot of a fibre coated for 31 s. The values of tensile strength and Weibull parameter ($m = 3$) are nearly equal to those of the fibre after heat-treatment cleaning; thus, the presence of crystalline SiC deposited in the form of tiny crystallites has no evident effect on the mechanical characteristics (see Table VI).

4. Conclusion

The role that chemical reactions between the substrate and the gas phase play in CVD processes is often ignored. In this work, we have presented experimental evidence for the occurrence of a reaction between silicoaluminate fibres and chloride compounds–H_2 mixtures. Attempts were made to produce a diffusion barrier coating of SiC which could serve simultaneously as a non-chemically interacting interface layer on aluminosilicate fibres of Nextel type which would enable the fibres to be used for reinforcing oxide-type matrices. A direct CVD on the fibres from $SiCl_4$–CH_4–H_2, MTS–H_2 and DDS–H_2 mixtures leads to brittleness and a loss of mechanical properties to a considerable extent. At the short CVD times characteristic of these experiments, the main conclusions of the thermodynamic study are partly corroborated by the experimental data. A β-SiC coating on the fibres is obtained, but it appears that the deposit is constituted of an SiC–C mixture and it is discontinuous or porous. With such a coating texture, the attack of the filaments with $AlCl_3$ loss remains important and leads to the brittleness of the fibre. The best results are obtained

TABLE VI Mechanical properties of Nextel-312, after each successive stage of CVD treatment until the final coating of SiC

	Rupture strength (MPa)	Young's modulus (GPa)	Weibull parameter
Nextel-312	1480	95	3.6
Air treatment, 1323K, 28 sec	1150	120	2.2
After SiC coating	800	120	3.4

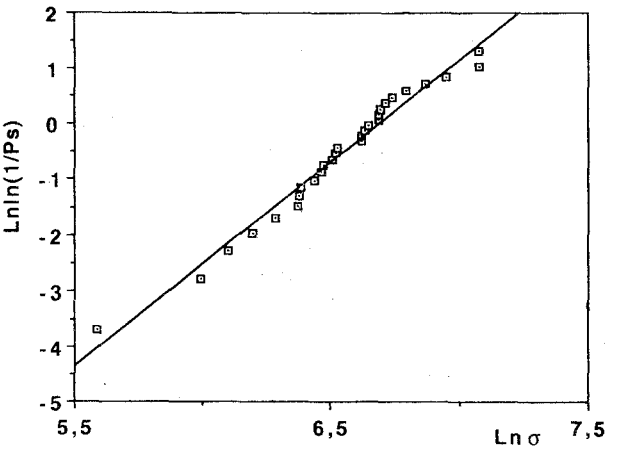

Figure 17 Weibull plots of Nextel-312 fibre after heat cleaning at 1050 °C and coating from the DDS–H_2 mixture at 1270 K for 31 s.

with the DDS–H_2 precursor, the loss of tensile strength being about 50%.

References

1. J. C. VIALA, J. BOUIX, H. VINCENT, J. L. PONTHENIER, J. DAZORD and C. VINCENT, Fr. Pat. 86 17 157 (4/11/86).
2. *Idem*, Fr. Pat. 89 04 660 (4/4/89).
3. H. VINCENT, J. L. PONTHENIER, C. VINCENT and J. BOUIX, *J. Cryst. Growth* **92** (1988) 553.
4. H. VINCENT, J. L. PONTHENIER, J. BOUIX, H. MOURICHOUX and C. VINCENT, *J. Phys. Suppl.* 5 **50** (1989) 249.
5. J. BOUIX, C. VINCENT, H. VINCENT and R. FAVRE, Materials Research Society, Symposium Proceedings 168, "Chemical Vapour Deposition of Refractory Metals and Ceramics", edited by T. M. Besman, B. M. Gallois, (MRS, Pittsburgh, PA, 1990) p. 305.
6. H. VINCENT, C. VINCENT, J. BOUIX, T. S. KANNAN, submitted.
7. T. S. KANNAN, J. DUBOIS and G. FANTOZZI, unpublished work.
8. J. KEARBY, *J. Amer. Chem. Soc.* **58** (1936) 374.
9. J. W. FAUST Jr, in "Silicon Carbide- 1973", edited by R. C. Marshall, J. W. Faust Jr and C. E. Ryan (University of South Carolina Press, Columbia, SC, 1974) p. 668.
10. H. G. SOWMAN and D. D. JOHNSON, *Ceram. Engng Sci. Proc.* **6** (9–10) (1985) 1221.
11. A. C. JENKINS and G. F. CHAMBERS, *Ind. Engng Chem.* (1987) 2367.
12. J. SCHLICHTING, *Powder Met. Int.* **12** (1980) 141.
13. *Idem, ibid.* **12** (1980) 196.
14. R. C. MARSHALL "Silicon carbide" (University South Carolina Press, Columbia, SC, 1974) p. 3.
15. K. E. SPEAR, *Pure Appl. Chem.* **54** (1982) 1297.
16. M. TUKPIN and A. ROBERT, *Proc. Brit. Ceram. Soc.* **22** (1973) 337.
17. A. I. KINGON, L. J. LUTZ, P. LIAW and R. F. DAVIS, *J. Amer. Ceram. Soc.* **66** (1983) 558.
18. F. CRISTIN, R. NASLAIN and C. BERNARD, in "Proceedings of the 7th International Conference on CVD", Los Angeles, October 1979, edited by T. O. Sedwick and H. Lydtin (The Electrochemical Society, Princeton, 1979) p. 499.
19. JANAF Thermochemical tables, 2nd Edn NSRDS-NBS 37 (National Bureau of Standards, U.S. Government Printing Office, Washington, DC, 1982).
20. J. C. VIALA, P. FORTIER and J. BOUIX, *Ann. Chim. Fr.* **11** (1986) 235.
21. Z. INOUE, Y. INOMATA and J. TANAKA, *J. Mater. Sci.* **15** (1980) 255.
22. Y. LARRERE, B. WILLER, J. M. LIHRMANN and M. DAIRE, *Rev. Int. Hautes Temp. Refract.* **21** (1984) 3.
23. B. L. KIDWELL, L. L. ODEN and R. A. McCUNE, *J. Appl Crystallogr.* **17** (1984) 481.
24. A. R. HOLTZ and M. F. GRETHER, "High Temperature Properties of Three NEXTEL Fibres" 32nd International SAMPE Symposium and Exhibition, Anaheim Convertion Centre, April 6–9, 1987 (3M Center, St Paul, MN).
25. M. GORMAN and S. A. SOLIN, *Solid State Commun.* **15** (1974) 761.
26. S. VEPREK, Z. IQBAL, H. R. OSWALD and A. P. WEBB, *Phys. Rev.* **C14** (1981) 295.

Received 26 June 1991
and accepted 7 February 1992